Journal of Radioanalytical and Nuclear Chemistry (2019) 320:71–78
https://doi.org/10.1007/s10967-019-06444-6

# Fast and accurate simultaneous quantification of strontium-90 and yttrium-90 using liquid scintillation counting in conjunction with the Bateman equation

**Kevin John Swearingen**[1] · **Nathalie A. Wall**[1]

Received: 19 October 2018 / Published online: 6 February 2019


**Abstract**
A derivation of the Bateman equation combined with successive liquid scintillation counting measurements was used to rapidly determine accurate individual activities of $^{90}$Sr and $^{90}$Y in samples containing both isotopes regardless of the sample age. This method does not require chemical separation of Sr from Y or waiting for secular equilibrium to take place. Accurate data can be obtained within 3 half-lives of $^{90}$Y ingrowth (i.e. within 5 days), associated uncertainties with this method are comparable to those obtained with traditional techniques that include separations. This novel technique allows for decreased sample processing cost and time, without reducing data quality.

**Keywords** Bateman equation · Sr-90 · Y-90 · Liquid scintillation

## Introduction

Strontium-90 and its daughter, $^{90}$Y, have a similar cumulative fission yield of approximately 6% [1]. The high yield and the longer half-life of $^{90}$Sr (28.8 years) make this isotope valuable for nuclear forensics applications [2–7]. Additionally, ingested $^{90}$Sr can replace Ca in bone and teeth, due to the chemical similarities between Sr and Ca. Accordingly, $^{90}$Sr is also important for environmental monitoring [8–12].

Strontium-90 is a pure $\beta^-$ emitter (0.546 MeV); $^{90}$Y is also a $\beta^-$ emitter (2.281 MeV) and its $\gamma$ emission (1.578 MeV) with the minute branching ratio of $1.4\times10^{-6}$ % makes it also essentially a pure $\beta^-$ emitter. Due to the lack of $\gamma$ or $\alpha$ emissions, $^{90}$Sr and $^{90}$Y are typically quantified via liquid scintillation counting (LSC). The wide energy distribution of $\beta^-$ decay and the lack of accurate peak discrimination with LSC prevent $^{90}$Sr and $^{90}$Y from being individually quantified when both are present in a sample. Several techniques are available to compensate for this problem. Common practices for the chemical separation of Sr from Y, in solutions that do not contain other radionuclides, include precipitation, solid phase extraction, or liquid–liquid extraction; $^{90}$Sr and $^{90}$Y are quantified separately following separation. Yttrium-90 ingrowth can also be measured in the $^{90}$Sr sample following separation [13–23]. Another technique relies on the higher energy $\beta^-$ decay of $^{90}$Y and resolving its activity using Cherenkov counting—the energy of the $\beta^-$ decay of $^{90}$Sr is too small to cause significant Cherenkov emissions. LSC can be used to determine the total sample activity and $^{90}$Sr activity is calculated from the difference between the LSC data and the Cherenkov counting of $^{90}$Y [24–31].

This present study demonstrates the quantification of the activities of both $^{90}$Sr and $^{90}$Y in a liquid sample that do not contain other radionuclides, without sample treatment or lengthy wait, taking advantage of secular equilibrium properties of the two radioisotopes and using a derivation of the Bateman equation [32].

## Experimental

### Reagents

Reagent grade chemicals were obtained from Sigma Aldrich (St. Louis, MO), JT Baker (Center Valley, PA), Thermo Fisher (Waltham, MA), and Alfa Aesar (Ward Hill, MA). Single element aqueous phase ICP standards were purchased from Inorganic Ventures (Christiansburg, VA) and single

✉ Nathalie A. Wall
nawall@wsu.edu

[1] Department of Chemistry, Washington State University, Pullman, WA 99163, USA

element organic phase ICP standards were purchased from VHG Labs (Manchester, NH). Strontium-90 radiotracer was purchased through the National Isotope Development Center (Oak Ridge, TN) and was received from Pacific Northwest National Laboratory (Richland, WA). Thenoyltrifluoroacetone (TTA) and 2-ethylhexylphosphonic acid mono-2-ethylhexyl ester (HEHEHP) were purified according to the literature [33, 34], all other reagents were used without purification.

## Instrumentation

Stable isotope concentrations of Sr and Y in liquid samples (aqueous and organic phases) were quantified via ICP-OES using an Agilent 5100 SVDV ICP-OES, equipped with an SPS 3 autosampler with a 1.3 mm interior diameter inert PTFE sleeved probe, using the software ICP Expert Version 7.1.0.6821 (Agilent Technologies, Santa Clara, CA) [35]. The instrument set-up conditions for aqueous and organic sample analyses are detailed in Table 1. The instrument was calibrated with NIST Traceable ICP-OES standards. For aqueous solution analyses, Inorganic Ventures Sr and Y standards in 2% $HNO_3$ were prepared as a multi-element cocktail via gravimetrically diluted in 2% $HNO_3$. Organic solution analyses used VHG Labs single element Sr and Y standards in hydrocarbon oil prepared as multi-element cocktail via gravimetric dilution in $10^{-2}$ M HDEHP in dodecane. For ICP-OES sample analysis, 1 mL aliquot of aqueous phase was diluted prior to analysis with 3 mL 2% $HNO_3$ and 1 mL aliquot of organic phase was diluted with 3 mL $10^{-2}$ M HDEHP in dodecane.

Radioactive isotopes of Sr and Y were quantified with a Beckman LS 6500 scintillation counter (Beckman Coulter, Brea, CA) using Ecoscint Original scintillating cocktail (National Diagnostic, Atlanta, GA). The counting window was set for all channels to be open and count times were either 5 or 20 min, depending on the sample activity. A volume of 0.5 mL of each sample was diluted with 19.5 mL of Ecoscint scintillation fluid in 20 mL vials, for optimum counting efficiencies. This large volume of scintillation fluid was used in order to enhance the detection of the high energy $^{90}Y$ $\beta^-$. With this geometry, efficiencies for both $^{90}Sr$ and $^{90}Y$ are approximately 99% [36]. All counting data were corrected for background.

## Bateman derived counting technique

Secular equilibrium applies to a system in which the parent has a much larger half-life than the daughter and is a state achieved when parent and daughter isotopes have reach equal activities. In particular, the ratio of the decay rates follows the criterion shown in Eq. 1 [37].

$$\frac{\lambda_{parent}}{\lambda_{daughter}} \leq \sim 10^{-4} \quad (1)$$

**Table 1** Instrumental operating conditions for the ICP-OES used in the analysis of stable aqueous and organic samples

| | Aqueous solutions | Organic solutions |
|---|---|---|
| Torch | 1.8 mm injector, one piece Torch Agilent G8010-60228 | 1.4 mm injector, demountable Torch Agilent G8010-60233 |
| Spray chamber | Twister Spray Chamber with helix, Glass Expansion 20-809-9199HE | |
| Nebulizer | SeaSpray 2 mL/min Glass expansion A14-07-USS2 | Conikal 2 mL/min Glass expansion A14-07-UC2 |
| Pump tubing material | PVC | Solva Flex |
| Sample pump speed (rpm) | 12 | 12 |
| Uptake delay (s) | 25 | 30 |
| Rinse time (s) | 30 | 40 |
| Read time (s) | 5 | 5 |
| RF Power (kW) | 1.20 | 1.20 |
| Stabilization time (s) | 15 | 15 |
| Viewing mode | SVDV* | SVDV* |
| Viewing height (mm) | 8 | 8 |
| Nebulizer flow (L/min) | 0.7 | 0.7 |
| Plasma flow (L/min) | 13 | 12 |
| Aux flow (L/min) | 0 | 1 |

**SVDV* synchronous vertical dual view

The half-life of $^{90}$Sr and $^{90}$Y are 28.8 years and 2.67 days, respectively; accordingly, the decay rate constant ratio between parent and daughter is $2.54 \times 10^{-4}$, within the definition of secular equilibrium. With the assumption that the sample is isotopically pure, (i.e. it is composed of only $^{90}$Sr and $^{90}$Y) the total activities can be calculated according to Eq. 2 (for time zero) and 3 (for any time).

$$A^0_{tot} = A^0_{Sr} + A^0_Y \tag{2}$$

$$A_{tot} = A_{Sr} + A_Y \tag{3}$$

Using Eq. 2, we define the initial ratio of $^{90}$Sr to total initial activity as Eq. 4

$$x = A^0_{Sr}/A^0_{tot} \tag{4}$$

We use this ratio to define the initial activities of $^{90}$Sr and $^{90}$Y in terms of the initial total activity (Eqs. 5 and 6).

$$A^0_{Sr} = x \cdot A^0_{tot} \tag{5}$$

$$A^0_Y = (1-x) \cdot A^0_{tot} \tag{6}$$

We express the number of atoms, N (Eq. 7), as a function of the initial activity equations (Eqs. 8 and 9).

$$A = \lambda \cdot N \tag{7}$$

$$N^0_{Sr} = \frac{x \cdot A^0_{tot}}{\lambda_{Sr}} \tag{8}$$

$$N^0_Y = \frac{(1-x) \cdot A^0_{tot}}{\lambda_Y} \tag{9}$$

The Bateman Equation accounts for the number of atoms of a parent and its daughter (in this case, $^{90}$Sr and $^{90}$Y) as defined with Eqs. 10 and 11, respectively [32, 37].

$$N_{Sr} = N^0_{Sr} \cdot e^{-\lambda_{Sr} \cdot t} \tag{10}$$

$$N_Y = \frac{\lambda_{Sr}}{\lambda_Y - \lambda_{Sr}} \cdot N^0_{Sr} \cdot \left(e^{-\lambda_{Sr} \cdot t} - e^{-\lambda_Y \cdot t}\right) + N^0_Y \cdot e^{-\lambda_Y \cdot t} \tag{11}$$

The initial quantities of Sr and Y are unknown and we substitute Eqs. 8 and 9 into Eqs. 10 and 11; we express the initial number of atoms in terms of initial total activity—measureable via LSC—leading to Eqs. 12 and 13. We further simplify Eqs. 13 to 14.

$$N_{Sr} = \left(\frac{x \cdot A^0_{tot}}{\lambda_{Sr}}\right) \cdot e^{-\lambda_{Sr} \cdot t} \tag{12}$$

$$N_Y = \frac{\lambda_{Sr}}{\lambda_Y - \lambda_{Sr}} \cdot \left(\frac{x \cdot A^0_{tot}}{\lambda_{Sr}}\right) \cdot \left(e^{-\lambda_{Sr} \cdot t} - e^{-\lambda_Y \cdot t}\right) + \left(\frac{(1-x) \cdot A^0_{tot}}{\lambda_Y}\right) \cdot e^{-\lambda_Y \cdot t} \tag{13}$$

$$N_Y = \left(\frac{x \cdot A^0_{tot}}{\lambda_Y - \lambda_{Sr}}\right) \cdot \left(e^{-\lambda_{Sr} \cdot t} - e^{-\lambda_Y \cdot t}\right) + \left(\frac{(1-x) \cdot A^0_{tot}}{\lambda_Y}\right) \cdot e^{-\lambda_Y \cdot t} \tag{14}$$

LSC measurements provide measured total solution activities; we convert Eqs. 12 and 14 to activities using Eq. 7, leading to Eqs. 15 and 16.

$$A_{Sr} = x \cdot A^0_{tot} \cdot e^{-\lambda_{Sr} \cdot t} \tag{15}$$

$$A_Y = \left(\frac{x \cdot A^0_{tot}}{\lambda_Y - \lambda_{Sr}}\right) \cdot \left(e^{-\lambda_{Sr} \cdot t} - e^{-\lambda_Y \cdot t}\right) \cdot \lambda_Y + (1-x) \cdot A^0_{tot} \cdot e^{-\lambda_Y \cdot t} \tag{16}$$

The sample is isotopically pure and we use Eq. 3 to combine Eqs. 15 and 16; we obtain Eq. 17.

$$A_{tot} = x \cdot A^0_{tot} \cdot e^{-\lambda_{Sr} \cdot t} + \left(\frac{x \cdot A^0_{tot}}{\lambda_Y - \lambda_{Sr}}\right) \cdot \left(e^{-\lambda_{Sr} \cdot t} - e^{-\lambda_Y \cdot t}\right) \cdot \lambda_Y + (1-x) \cdot A^0_{tot} \cdot e^{-\lambda_Y \cdot t} \tag{17}$$

This equation has three unknown parameters: the initial total activity, $A^0_{tot}$, the final total activity, $A_{tot}$, and the ratio, $x = A^0_{Sr}/A^0_{tot}$. Over the course of several days (2–21 days), we measure (LSC) multiple times the sample activity containing $^{90}$Sr and its growing daughter $^{90}$Y. The counts and the times at which they occur are plotted in the software OriginPro 2015, defining the first count as $A^0_{tot}$ occurring at $t = 0$. This plot for measured total activity as a function of time is then fitted with a non-linear curve fit. The curve fitting and Eqs. 5 and 6 provide the $x$ ratio for the initial measured activity and we quantify the initial $^{90}$Sr and $^{90}$Y activities using the measured total initial activity.

## Method validations

In method validation, we disrupted the secular equilibrium of a $^{90}$Sr/$^{90}$Y solution using solvent extraction, to quantify the individual Sr and Y concentrations using our fitting equation. A solution of $10^{-5}$ M Sr and $10^{-5}$ M Y in 0.1 M $NaClO_4$ buffered at pH 5.5 with 1 mM MES buffer was spiked with a $^{90}$Sr/$^{90}$Y solution that had reach secular equilibrium, to obtain an activity of approximately 250 Bq/mL. This solution was contacted with equal volume of $10^{-2}$ M HEHEHP in dodecane for 2 h (determined to be a sufficient time to reach equilibrium) on an orbital shaker.

HEHEHP will preferentially extract trivalent Y into the organic phase, leaving the Sr in the aqueous phase, shifting both organic and aqueous phases away from secular equilibrium in opposite directions. The biphasic samples were then centrifuged for 5 min at 3000 rpm and 0.5 mL aliquots of each phases were added to 19.5 mL of Ecoscint Original. These new samples were counted (LSC) daily for 22 days. At 22 days, the samples will have achieved secular equilibrium and we use the measured activity beyond that point to calculate the specific $^{90}$Sr and $^{90}$Y activities to compare to the curve fitting technique. A sample of aqueous solution similar to that above and without any contact with an organic phase was also measured multiple times over the same 22-day period.

In a second method validation, we compared results obtained using a $^{90}$Sr/$^{90}$Y solution and our fitting equation with data obtained using stable Sr and Y and direct concentration measurements. The second validation technique consisted of a solvent extraction study with variable TTA concentration; one experiment was conducted using $^{90}$Sr and $^{90}$Y radioisotopes and the second experiment employed stable Sr and Y. In this case, we are again aiming at disturbing the secular equilibrium between $^{90}$Sr and $^{90}$Y, as Y and Sr form complexes with ligands, but of different strength. This technique sought to compare the distribution coefficient for each element (as a radioisotope or a stable isotope) between an organic phase and aqueous phase, providing a means to compare the Bateman-derived technique with stable element ICP-OES analysis. The total activities of the radiotracer samples were measured using LSC and individual activity of $^{90}$Sr and $^{90}$Y were calculated using the Bateman equation; stable Sr and Y respective concentrations were measured using ICP-OES. The resulting ligand extraction mechanism from both experiment sets (radiotracer and stable isotopes) were then compared. Stable isotope samples contained an aqueous phase of $10^{-5}$ M Sr and $10^{-5}$ M Y in 0.09 M $NaClO_4$ with 0.01 M acetate buffer at pH 4, the organic phases consisted of 0.02–0.1 M TTA in xylenes; the two phases were of equal volumes. The two phases were contacted for 2 h on an orbital shaker, centrifuged for 5 min at 3000 rpm, and 1 mL aliquots of each phase were sampled for ICP–OES analysis. The organic stable aliquots were diluted with $10^{-2}$ M HDEHP in dodecane and analyzed using ICP-OES [35]; the aqueous stable aliquots were diluted with 2% $HNO_3$ and analyzed with ICP-OES [35]. The radiotracer studies consisted of an aqueous phase containing 150 Bq/mL $^{90}$Sr + $^{90}$Y, in presence of stable Sr and Y ($10^{-5}$ M Sr and $10^{-5}$ M Y), 0.09 M $NaClO_4$, with 0.01 M sodium acetate as buffer at pH 4, the organic phases consisted of 0.02–0.1 M TTA in xylenes; the two phases were of equal volumes. Radiotracer aliquots (0.5 mL) of each phase were added to 19.5 mL of Ecoscint Original and counted for 5 min several times over the course of 3 days. The diluted TTA does not lead to quenching during counting. The distribution coefficients were calculated using Eq. 18, where $[M]_{(org)}$ and $[M]_{(aq)}$ are the concentration of the element in the organic phase and in the aqueous phase, respectively. We plotted these calculated values as a function of the TTA concentration.

$$D = \sum [M]_{(org)} \Big/ \sum [M]_{(aq)} \tag{18}$$

## Results and discussion

### Curve fitting results

Using the first method validation dataset (using the extractant HEHEHP), we counted (LSC) daily for 22 days the aqueous and organic phase aliquots from one sample and the uncontacted aqueous aliquot. Data are presented with Fig. 1.

Figure 1 shows that the uncontacted aqueous phase had not quite reached secular equilibrium at the time when we prepared the sample; this was most likely due to the tracer being acidified immediately prior to use and the time between acidifying and spiking the solution was not adequate for both the $^{90}$Sr and $^{90}$Y to completely dissolve in solution. In addition, the organic phase contains both $^{90}$Sr and $^{90}$Y, with $^{90}$Y accounting for the majority of the activity; this is shown by the decrease in total activity (12–7 Bq). Finally, the aqueous phase consists primarily of $^{90}$Sr and the later counts show the ingrowth of $^{90}$Y as secular equilibrium

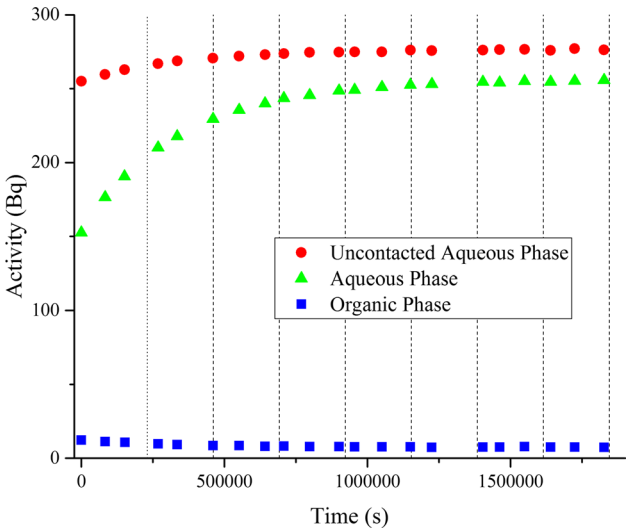


**Fig. 1** Activities of organic (blue squares) and aqueous phases (green triangles) from containing $10^{-5}$ M Sr, $10^{-5}$ M Y, and 250 Bq/mL of $^{90}$Sr/$^{90}$Y, contacted with $10^{-2}$ M HEHEHP in dodecane at pH 5.5; the red circles are an aliquot of uncontacted aqueous phase to show initial activity, and the dashed lines represent each consecutive $^{90}$Y half-life. (Color figure online)

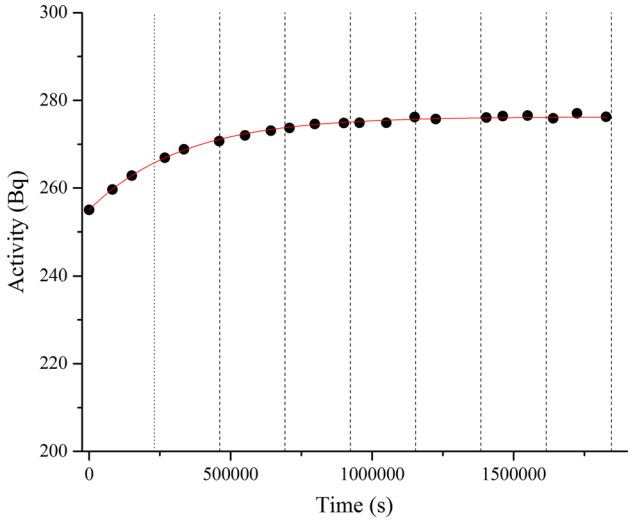


**Fig. 2** Non-linear curve fit for the uncontacted aqueous phase containing $10^{-5}$ M Sr, $10^{-5}$ M Y, and 250 Bq/mL of $^{90}$Sr/$^{90}$Y; the dashed lines represent each consecutive $^{90}$Y half-life

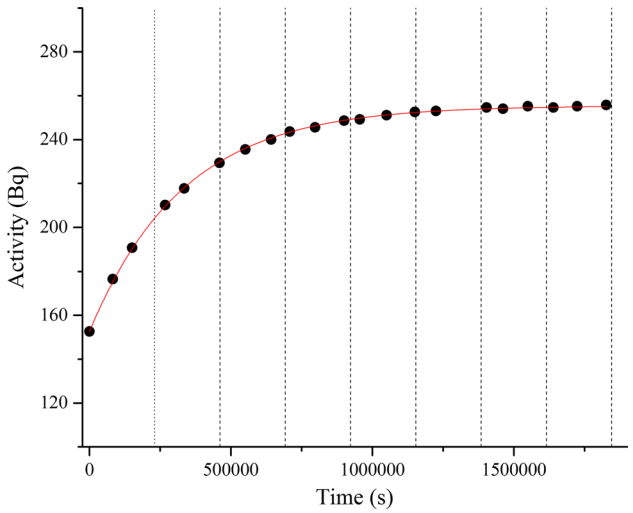


**Fig. 3** Non-linear curve fit for the aqueous phase containing $10^{-5}$ M Sr, $10^{-5}$ M Y, and 250 Bq/mL of $^{90}$Sr/$^{90}$Y after contact with $10^{-2}$ M HEHEHP in dodecane; the dashed lines represent each consecutive $^{90}$Y half-life

is achieved. We can attribute the loss of Y at the early stage of the experiment to the formation of a third phase, which does not impact the validity of the procedure.

We fitted Eq. 17 using OriginPro 2015's nonlinear curve fit to each of the three data sets shown in Fig. 1, to obtain the exact $^{90}$Sr-to-Total activity ratio (x, as shown in Eq. 4). The resulting curve fits are shown with Figs. 2, 3, and 4.

Table 2 presents the calculated $x$ ratio and associated fit coefficient of determination for each data set. The individual initial activities for $^{90}$Sr and $^{90}$Y can be quantified using the

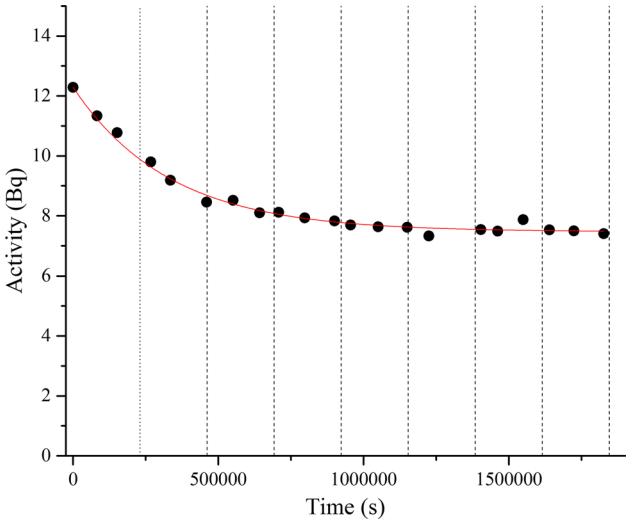


**Fig. 4** Non-linear curve fit for the $10^{-2}$ M HEHEHP in dodecane phase, after contacting the aqueous phase containing $10^{-5}$ M Sr, $10^{-5}$ M Y, and 250 Bq/mL of $^{90}$Sr/$^{90}$Y; the dashed lines represent each consecutive $^{90}$Y half-life

**Table 2** Values for $x$ ratio ($^{90}$Sr-to-Total activity ratio) and fit coefficient of determination ($R^2$) calculated for data sets shown in Figs. 2, 3, and 4

| Phase | Uncontacted aqueous | Contacted aqueous | Contacted organic |
|---|---|---|---|
| $x$ | 0.542 | 0.838 | 0.304 |
| $R^2$ | 0.997 | 0.999 | 0.990 |

$x$ ratio values and the initial total activities determined with LSC. While the extraction system used for this study was not optimized for optimum extraction, data show that the Bateman derivation is a good fit for the $^{90}$Sr/$^{90}$Y behavior ($R^2 \geq 0.99$), regardless of the initial ratio.

## First method validation

For the first method validation, we had prepared samples containing stable Sr and Y ($10^{-5}$ M each) and a spike of a $^{90}$Sr/$^{90}$Y solution that had reach secular equilibrium. This aqueous solution was equilibrated with $10^{-2}$ M HEHEHP in dodecane and an aliquot of each phase was sampled for successive LSC counting over 22 days—all counting data were corrected for background. Data were fitted with Eq. 17. The fitting function provided $x$ ratio values for each sample. We used the measurements at 22 days as final activities—after 22 days, the samples will have achieved secular equilibrium and 50% of the activity will come from $^{90}$Sr and 50% from $^{90}$Y.

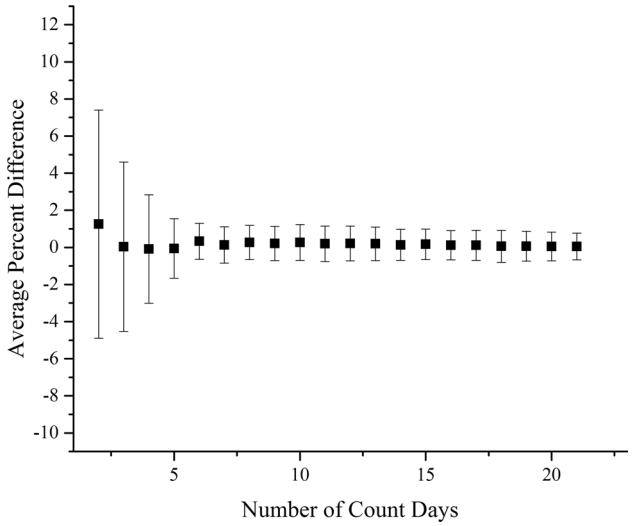


**Fig. 5** Average percent difference between the ratio $x$ ($^{90}$Sr to total activity ratio) calculated via the Bateman derivation curve fitting function and from the final secular equilibrium (day 22) plotted versus the number of count days, uncertainty was calculated as the standard deviation of triplicate samples

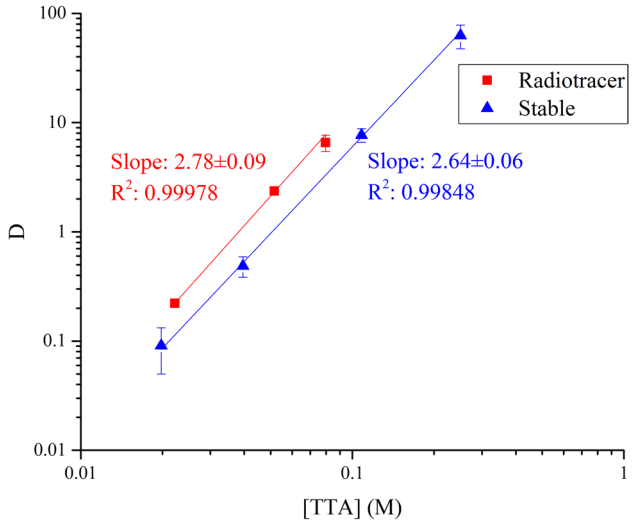


**Fig. 6** Comparison of ligand-dependence slope analysis studies for spiked and stable solutions of $10^{-5}$ M Y and $10^{-5}$ M Sr in 0.1 M $NaClO_4$ buffered at pH 5.5 with 1 mM MES buffer contacting $10^{-2}$ M HEHEHP in dodecane. Spiked solution concentrations were quantified using the Bateman derived curve fitting and stable solutions were quantified using ICP-OES data. Uncertainties were calculated as 2 times the standard deviation of triplicate samples

To gauge the precision of the curve fitting technique, the ratios calculated from the final counts (day 22) were compared to the ratios calculated with each set of count data as it was fitted with the function. We calculated the percent differences between the curve fit calculated x-values and the 22-day $x$-values. Figure 5 presents such percent difference for the average obtained with nine separate samples; the percent difference is plotted as a function of the number of count days (i.e. at 5 count days, the samples had been counted on 5 separate consecutive days).

Figure 5 shows that the average percent different is constant and close to 0 over the whole time range, but with larger uncertainties during the first four days. Even after only 2 count days, the average percent difference is $< 2\%$. Counting over the course of 6 days decreases the average percent difference to zero with a standard deviation of less than 1. Typically, counting methods (without separations) require the samples to achieve secular equilibrium before an accurate value can be determined (as here, at day 22). Being able to gain an approximate value in 2 days and an accurate value in less than 1 week is a drastic improvement, compared to the necessary 3 weeks required to reach secular equilibrium.

## Second method validation

For the second validation we had prepared two sets of extraction samples, using variable TTA concentrations; one set employed $^{90}$Sr and $^{90}$Y radioisotopes (quantified with LSC) added to stable Sr and Y, while the second experiment set employed exclusively stable Sr and Y (quantified with ICP-OES). The individual Sr and Y radiotracer concentrations were derived using the Bateman curve fitting function and the stable Sr and Y concentrations were quantified using ICP-OES for both the aqueous and organic phases. The distribution coefficients, D, were plotted as a function of TTA concentration as shown with Fig. 6. Under the conditions of this study, no significant concentrations of Sr were detected in the organic phase in either experiment. We observed a shift of D values between the stable and radiotracer sample sets. This difference is potentially due to differences between the aqueous phases. The radiotracer spike of $^{90}$Sr/$^{90}$Y was in $HClO_4$ to ensure the Sr and Y stayed in solution without sorbing to the vial. After the addition of the radiotracer, the solution had to be brought back to pH 4 with NaOH. With the addition of NaOH, there may have been localized hydrolysis that occurred with the Y. Overall though, the Bateman derived concentration values based on LSC data provided a similar trend compared to the study conducted with stable metals and ICP-OES quantification.

Under acidic conditions ($pH \leq 2$), the ligand dependent slope of TTA has a slope equal to the charge of the metal being extracted; extractions of trivalent metals such as Y exhibit a slope of 3. When the pH is increased above 2, the slope of the ligand dependence plot gradually decreases. This change is believed to be partially due to the increase in the aqueous phase solubility of TTA as pH increased. The slopes of both the stable and radiotracer experiments were similar to those reported in the literature [34].

## Conclusion

This work demonstrate that a Bateman derived fit developed in this paper provides accurate quantification of each $^{90}$Sr and $^{90}$Y in solutions that are not in secular equilibrium. This method has the advantage of providing data as accurate as traditional methods, but without costly and time-consuming elemental separation and data are obtained within a very short time (5 day counting).

**Acknowledgements** This work was supported by the Defense Threat Reduction Agency, Basic Research Award #HDTRA1-12-1-0015, to Washington State University.

## References

1. Chadwick MB, Herman M, Oblozinsky P et al (2011) ENDF/B-VII. 1 nuclear data for science and technology: cross sections, covariances, fission product yields and decay data. Nucl Data Sheets 112:2887–2996
2. Baum EM, Ernesti MC, Knox HD, Miller TR, Watson AM (2009) Nuclides and isotopes chart of the nuclides, 17th edn. Knolls Atomic Power Laboratory
3. Bowen WQ, Cottee M, Hobbs C (2012) Multilateral cooperation and the prevention of nuclear terrorism: pragmatism over idealism. Int Aff 88:349–368
4. Charbonneau L, Benoit J-M, Jovanovic S et al (2014) A nuclear forensic method for determining the age of radioactive cobalt sources. Anal Methods 6:983–992
5. Eby N, Hermes R, Charnley N, Smoliga JA (2010) Trinitite-the atomic rock. Geol Today 26:180–185
6. Fedchenko V (2014) The role of nuclear forensics in nuclear security. Strateg Anal 38:230–247
7. Jones AE, Turner P, Zimmerman C, Goulermas JY (2014) Classification of spent reactor fuel for nuclear forensics. Anal Chem 86:5399–5405
8. Boulyga SF (2011) Mass spectrometric analysis of long-lived radionuclides in bio-assays. Int J Mass Spectrom 307:200–210
9. Boulyga SF, Becker JS (2002) Isotopic analysis of uranium and plutonium using ICP-MS and estimation of burn-up of spent uranium in contaminated environmental samples. J Anal At Spectrom 17:1143–1147
10. Public health statement: strontium. https://www.atsdr.cdc.gov/ToxProfiles/tp159-c1-b.pdf. Accessed 1 Feb 2019
11. Froidevaux P, Geering JJ, Valley JF (2006) 90Sr in deciduous teeth from 1950 to 2002: the Swiss experience. Sci Total Environ 367:596–605
12. Mangano JJ, Gould JM, Sternglass EJ et al (2003) An unexpected rise in strontium-90 in US deciduous teeth in the 1990s. Sci Total Environ 317:37–51
13. Alvarez A, Navarro N, Salvador S (1995) New method for 90Sr determination in liquid samples. J Radioanal Nucl Chem 191:315–322
14. ASTM International (2013) ASTM D5811-08(2013) standard test method for strontium-90 in water. ASTM International, West Conshohocken
15. Wang JJ (2013) A quick liquid scintillation counting technique for analysis of 90Sr in environmental samples. Appl Radiat Isot 81:169–174
16. Environmental Protection Agency (2010) Rapid radiochemical methods for selected radionuclides in water for environmental restoration following homeland security events. Montgomery, AL
17. Grate JW, Strebin R, Janata J et al (1996) Automated analysis of radionuclides in nuclear waste: rapid determination of 90Sr by sequential injection analysis. Anal Chem 68:333–340
18. Holmgren S, Tovedal A, Jonsson S et al (2014) Handling interferences in 89Sr and 90Sr measurements of reactor coolant water: a method based on strontium separation chemistry. Appl Radiat Isot 90:94–101
19. Kameo Y, Katayama A, Fujiwara A et al (2007) Rapid determination of 89Sr and 90Sr in radioactive waste using Sr extraction disk and beta-ray spectrometer. J Radioanal Nucl Chem 274:71–78
20. Kiba T, Mizukami S (1958) Rapid separation of radioactive strontium extraction with TTA-hexone. Bull Chem Soc Jpn 31:1007–1013
21. Lee JS, Park UJ, Son KJ, Han HS (2009) One column operation for 90Sr/90Y separation by using a functionalized-silica. Appl Radiat Isot 67:1332–1335
22. Mateos JJ, Gomez E, Garcias F et al (2000) Rapid 90Sr/90Y determination in water samples using a sequential injection method. Sect Title Water 53:139–144
23. Maxwell SL, Culligan BK (2009) Rapid method for determination of radiostrontium in emergency milk samples. J Radioanal Nucl Chem 279:757–760
24. Holmgren S, Tovedal A, Björnham O, Ramebäck H (2016) Time optimization of 90Sr determinations: sequential measurement of multiple samples during ingrowth of 90Y. J Radioanal Nucl Chem 110:150–154
25. O'Hara MJ, Burge SR, Grate JW (2009) Automated radioanalytical system for the determination of Sr-90 in environmental water samples by Y-90 Cherenkov radiation counting. Anal Chem 81:1228–1237
26. Olfert JM, Dai X, Kramer-Tremblay S (2014) Rapid determination of 90Sr/90Y in water samples by liquid scintillation and Cherenkov counting. J Radioanal Nucl Chem 300:263–267
27. Pan J, Emanuele K, Maher E, Lin ZC, Healey S, Regan P (2016) Analysis of radioactive strontium-90 in food by Čerenkov liquid scintillation counting. Appl Radiat Isot 126:214–218
28. Tarancón A, Alonso E, Garc JF, Rauret G (2002) Sr/90 Y determination by Cerenkov, liquid scintillation and plastic scintillation techniques. Anal Chim Acta 471:135–143
29. Tayeb M, Dai X, Corcoran EC, Kelly DG (2014) Evaluation of interferences on measurements of 90Sr/90Y by TDCR Cherenkov counting technique. J Radioanal Nucl Chem 300:409–414
30. Tsroya S, Dolgin B, German U et al (2013) Fast determination of 90Sr/90Y activity in milk by Cherenkov counting. Appl Radiat Isot 82:332–339
31. Vaca F, Manjón G, Garcia-León M (1998) Efficiency calibration of a liquid scintillation counter for 90Y cherenkov counting. Nucl Instrum Methods Phys Res Sect A Accel Spectrom Detect Assoc Equip 406:267–275
32. Bateman H (1910) The solution of a system of differential equations occuring in the theory of radioactive transformations. Proc Cambridge Philos Soc Math Phys Sci 15:423–427
33. Zhengshui H, Ying P, Wanwu M, Xun F (1995) Purification of organophosphorus acid extractants. Solvent Extr Ion Exch 13:965–976
34. Friend MT, Wall NA (2017) Hafnium(IV) complexation with oxalate at variable temperatures. Radiochim Acta 105:379–388

35. Swearingen KJ, Omoto T, Wall N (2017) Analysis of organic and high dissolved salt content solutions using inductively coupled plasma optical emission spectrometry. J Anal At Spectrom 37:1231–1236
36. Eikenberg J, Beer H, Rüthi M, Zumsteg I, Vetter A (2006) Precise determination of Sr-89 and 90-Sr 90-Y in various metrics. The LSC 3-window approach. In: Chatupnik S, Schonhofer F, Noakes J (eds) LSC 2005, advances in liquid scintillation spectrometry, pp 237–249
37. L'Annunziata M (2012) Handbook of radioactivity analysis. Academic Press, London